

Decadal to millennial-scale solar forcing of Last Glacial Maximum climate in the Estancia Basin of central New Mexico



Kirsten M. Menking

Department of Earth Science and Geography, Vassar College, Poughkeepsie, NY 12604, USA

ARTICLE INFO

Article history:

Received 7 November 2014

Available online 25 February 2015

Keywords:

Solar-climate cycles

Last Glacial Maximum

Lake levels

Abrupt climate change

ABSTRACT

Lacustrine sediments from the Estancia Basin of central New Mexico reveal decadal to millennial oscillations in the volume of Lake Estancia during Last Glacial Maximum (LGM) time. LGM sediments consist of authigenic carbonates, detrital clastics delivered to the lake in stream flow pulses, and evaporites that precipitated in mudflats exposed during lake lowstands and were subsequently blown into the lake. Variations in sediment mineralogy thus reflect changes in hydrologic balance and were quantified using Rietveld analysis of X-ray diffraction traces. Radiocarbon dates on ostracode valve calcite allowed the construction of mineralogical time series for the interval ~23,600 to ~18,300 ka, which were subjected to spectral analysis using REDFIT (Schulz and Mudelsee, 2002). Dominant periods of ~900, ~375, and ~265 yr are similar to cycles in Holocene ^{14}C production reported for a variety of tree ring records, suggesting that the Lake Estancia sediments record variations in solar activity during LGM time. A prominent spectral peak with a period of ~88 yr appears to reflect the solar Gleissberg cycle and may help, along with the ~265 yr cycle, to explain an ongoing mystery about how Lake Estancia was able to undergo abrupt expansions without overflowing its drainage basin.

© 2015 University of Washington. Published by Elsevier Inc. All rights reserved.

Introduction

The lake level history for pluvial Lake Estancia in central New Mexico reveals ten abrupt millennial scale oscillations during and after Last Glacial Maximum (LGM) time (Fig. 1), followed by desiccation in the early Holocene (Allen and Anderson, 2000; Anderson et al., 2002). While the general cause of late Pleistocene lake expansion likely was increased precipitation associated with a southerly shift of the polar jet stream in response to Laurentide ice sheet growth (Kutzbach and Wright, 1985; Benson et al., 1990; Menking et al., 2004), the number and timing of Estancia highstands and lowstands remain largely unexplained. Anderson et al. (2002) described stratigraphic and radiocarbon evidence for lake expansion during the Younger Dryas, attributing lake rise to increased winter moisture from Pacific sources. Looking slightly farther back in time, Zhang et al. (2014) called on a reduction in strength of the East Asian summer monsoon and coincident southward shifts in position of the intertropical convergence zone (ITCZ) and polar jet stream to explain a rise in Lake Estancia at ~16.1 ka. Causes of still earlier oscillations have not been explored, though similar lake level variations have been observed for Lakes San Agustin in New Mexico (Phillips et al., 1992) and King in western Texas (Wilkins and Currey, 1997).

In addition to uncertainty about the climatic driver(s) of Estancia lake level oscillations, questions exist regarding the precipitation and temperature conditions required to generate different lake volumes.

Leopold (1951) estimated that highstands of Lake Estancia could be achieved with a 4.5°C annual temperature reduction combined with an increase in precipitation of 50% relative to modern conditions, values confirmed by numerical modeling experiments (Menking et al., 2004). However, while such conditions appear capable of raising Lake Estancia from its lowstand level to its highstand level, the amount of time required to do so (~300 yr) is greater than that available, as demonstrated by the sedimentary record (Fig. 2; Menking et al., 2004). Abrupt stratigraphic transitions from finely laminated gypsum to massive, bioturbated marl occur within 1–2 cm in LGM sediments, reflecting lake expansions that took place over a matter of decades to at most a century, according to radiocarbon age control (Allen and Anderson, 2000). In order for the lake to have risen this rapidly, modeling experiments show that precipitation must have increased by at least 75% over modern values, yet had such rates been sustained, Lake Estancia would have overshot its known highstand level and might even have overflowed its basin (Fig. 2; Menking et al., 2004).

Here I present evidence to resolve this conundrum, calling on variations in winter moisture modulated by solar activity to allow rapid expansions in lake level without corresponding overshoot. Spectral analysis of high resolution (1-cm sample interval, ~35 yr per sample) measurements of sediment mineralogy reveals decadal to millennial-scale periodicities that have been attributed to solar forcing (Damon and Jirikovic, 1992; Damon and Peristykh, 2000; Clemens, 2005). Similar cycles have been demonstrated in Pleistocene and Holocene records from other sites in New Mexico where they appear responsible for driving temperature-related changes in tree line (Jiménez-Moreno et al.,

E-mail address: kimenking@vassar.edu.

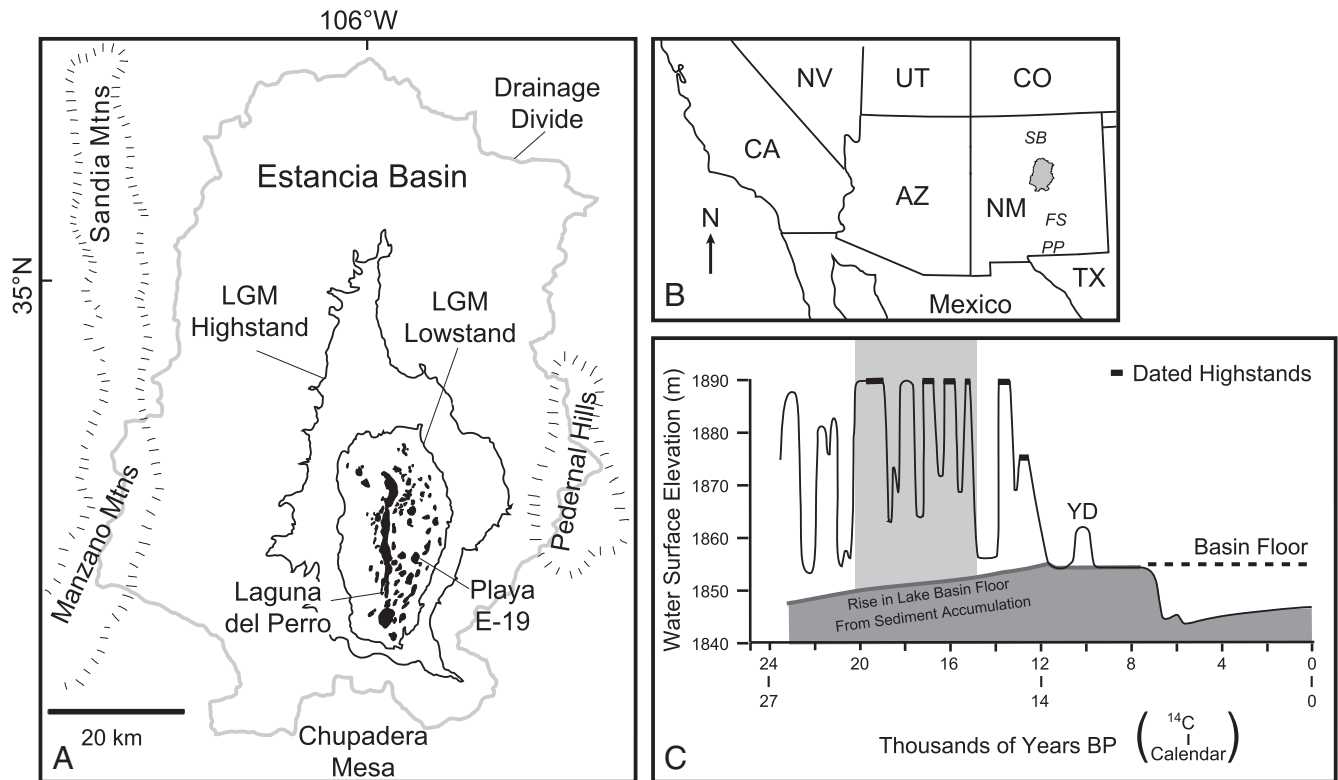


Figure 1. A) Map of the 5000 km² Estancia Basin in central New Mexico showing last Glacial Maximum (LGM) highstand (1100 km² lake surface area) and lowstand (400 km² lake surface area) shorelines as well as >80 playa basins (black areas enclosed by the lowstand shoreline) excavated during mid-Holocene drought. Samples for this study were acquired from the southwestern end of the Laguna del Perro playa, with additional age control from playa E-19. B) Map of the southwestern United States and northern Mexico showing the location of the Estancia basin (gray shaded area). CA = California, NV = Nevada, UT = Utah, CO = Colorado, AZ = Arizona, NM = New Mexico, TX = Texas, FS = Fort Stanton Cave, PP = Pink Panther Cave, SB = Stewart Bog. C) The lake level history for pluvial Lake Estancia shows ~10 highstand/lowstand oscillations during and after the LGM, the last highstand occurring during the Younger Dryas (YD). Mid-Holocene deflation during a two-stage drought excavated playa basins into the lake floor, exposing the late Pleistocene lacustrine stratigraphy. Wetter conditions in the later Holocene have subsequently led to a partial filling of these playas, resulting in a rise of the water table. The gray shading behind the lake level curve between ~15 and 20 thousands of years BP indicates the time period analyzed in this paper.

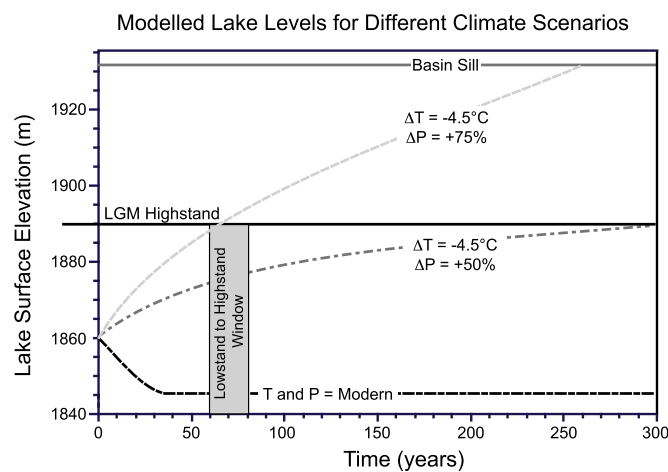


Figure 2. Numerical modeling results from Menking et al. (2004) reveal that Lake Estancia with an initial surface elevation equivalent to the known Pleistocene lowstand value (1860 m) would dry up (dashed black curve) under modern climatic conditions (T = temperature, P = precipitation). That same lake would fill to LGM highstand values (solid black line at 1890 m) in ~300 yr with an annual temperature reduction of 4.5°C and precipitation increase of 50% (dashed dark gray curve), as proposed by Leopold (1951), but stratigraphic evidence shows that the lake rose from lowstand to highstand elevations within 60–80 yr (Allen and Anderson, 2000), necessitating even greater amounts of precipitation. An increase in precipitation of 75% (dashed light gray curve) would have led the lake to achieve its known highstand within the time required by the stratigraphic evidence, but if sustained, would have led the lake to overflow its basin within ~250 yr (1932 m basin sill, solid dark gray line). The full range of model experiments can be found in Menking et al. (2004).

2008) as well as variations in precipitation abundance recorded in speleothem oxygen isotope values (Asmerom et al., 2007, 2010). Thus decadal to millennial solar forcing may have been a driver of rapid regional changes in winter moisture throughout the last 25,000 yr, a factor to be considered where drought is expected as human-induced climate change progresses (Ault et al., 2014).

Study area

Estancia Basin and its late Pleistocene lake (Fig. 1) are described extensively in the studies of Allen and Anderson (2000), Anderson et al. (2002), and Menking and Anderson (2003), and so will be described only briefly here. A centripetal drainage pattern fed Lake Estancia throughout the late Pleistocene, with a majority of runoff originating in the Manzano Mountains (Paleozoic clastics and carbonates) on the basin's western edge. Radiocarbon dated shoreline and basin center deposits show that the lake fluctuated in size between 400 and 1100 km² and ~5 and 45 m water depth (Allen and Anderson, 2000; Menking et al., 2004), and the termination of a majority of stream channels at highstand shorelines shows that while the lake was fed by stream flow during highstands, it was maintained primarily by groundwater during lowstands. The presence of several temporally distinct highstand shorelines at a common elevation (Fig. 1C) led Allen and Anderson (2000) to propose a leakage mechanism for the basin in which deep groundwater outflow might have matched rates of inflow when the lake grew to a particular volume.

Basin center deposits reveal that highstands of Lake Estancia were accompanied by influxes of detrital clastics washed into the lake from Paleozoic sedimentary rocks in the Manzano Mountains (Allen and

Anderson, 1993). During lowstands, sulfate-rich groundwater originating from solution of Permian gypsum and gypsiferous sandstone that underlies the basin discharged to the basin floor and led to the crystallization of gypsum in mudflats around the contracted lake. Sand-sized rhombs of gypsum show rounded edges, indicating wind transport from the mudflats into the lake (Allen and Anderson, 2000). Abundances of detrital clastics and gypsum thus serve as proxies for wetter and drier intervals throughout the late Pleistocene.

Basin center deposits were exposed by deflation during a two-stage drought that occurred from 7000–5400 ^{14}C yr BP (Menking and Anderson, 2003) and are readily accessible in more than 80 playa basins >10 m deep and >1 km² in area. The same stratigraphic units are found in each of these exposures, allowing a correlation throughout the basin. Measurements of oxygen isotopic composition on modern stream flow (average $\delta^{18}\text{O} = -10.8\% \pm 0.6\%$), groundwater (average $\delta^{18}\text{O} = -11.0\% \pm 0.2\%$), and precipitation (average winter $\delta^{18}\text{O} = -14.1\% \pm 0.6\%$, average summer $\delta^{18}\text{O} = -4.2\% \pm 1.3\%$) reveal that the Estancia basin is dominated by winter moisture (Menking and Anderson, 2003), and previous work showed that the mid-Holocene drought likely resulted from enhanced La Niña conditions that suppressed winter precipitation and associated groundwater recharge, thereby dropping the level of the water table and allowing deflation of the basin floor (Menking and Anderson, 2003). Summer precipitation is thought to have little influence on the basin's hydrologic balance given high rates of evapotranspiration in this semi-arid setting.

Methods

I conducted a high-resolution study of mineralogy (calcite, evaporites, and detrital clastics) in LGM sediments to look for evidence of decadal to millennial climatic change in the Estancia Basin. Samples were collected from the southeastern end of the Laguna del Perro playa (Fig. 1). Three vertically overlapping trenches were dug to expose the LGM sediments and to access less weathered materials (Fig. 3). The base of the sequence was identified from a dated marker bed exposed throughout the basin that contains a high concentration of the pelecypod *Pisidium* while the top was determined from an abrupt change in sediment color, mineralogy, and stratification associated with lake level decline at the end of the LGM (Bachhuber, 1971, called LGM

sediments the “E zone” and the overlying lake lowstand sediment package the “D zone”; Allen and Anderson, 2000). Additional distinctive stratigraphic layers (typically laminated gypsum) were used to correlate between the three trenches. Slabs of material 20–30 cm in length, 10 cm in width, and 10 cm deep were cut out of each trench, bagged, and transferred to Vassar College for analysis. In the lab, slabs were photographed and sampled at 1 cm intervals, and the samples were dried and ground to a fine powder with a mortar and pestle.

Random powder mounts of the ground samples were analyzed with a Bruker D2 Phaser X-ray diffractometer with a Lynxeye detector open to 4° and a variable rotation rate of 6 rotations per minute. The samples were scanned between 8° and 80° 2 θ with a step size of 0.02° and a scan rate of 1 s per step. Diffraction traces were imported into TOPAS-Academic software for Rietveld quantitative analysis (Bish and Howard, 1988; Bish and Post, 1993; Young, 1993). Crystallographic indices for calcite, gypsum, quartz, illite, kaolinite, montmorillonite, albite, anorthite, and orthoclase were acquired from Downs and Hall-Wallace (2003) and a database provided by Bruker. Due to a lab miscommunication, about a third of the samples were subjected to loss on ignition analysis (LOI) prior to X-ray diffraction. Heating the samples to 450°C for 2 h caused the conversion of gypsum to anhydrite, so the latter mineral was also included in the analysis. Anhydrite was found only in the samples that had been subjected to LOI.

Following the example of Bish and Post (1993), I prepared a number of binary mixtures of quartz, calcite, gypsum, and anhydrite in order to determine the accuracy of the Rietveld technique. Hand sample specimens of these minerals were crushed to sand and granule size using a jaw crusher, followed by grinding to fine powder in a Cole-Parmer analytical mill. Mixtures representing 50% by weight of each of two of the mineral standards were then created and subjected to the same X-ray diffraction and Rietveld analyses as the Lake Estancia samples.

Age control consists of radiocarbon dates on ostracode valves. Approximately 5 g of sediment from three 1-cm-thick intervals was disaggregated using a 5% sodium hexametaphosphate solution. The samples were then washed through 250, 125, and 63 μm sieves to get rid of clay and silt-sized particles. Sieve residues were dried and then picked for ostracodes using a vacuum extraction line containing a fine mesh screen. Picked ostracodes were rewashed in 5% sodium

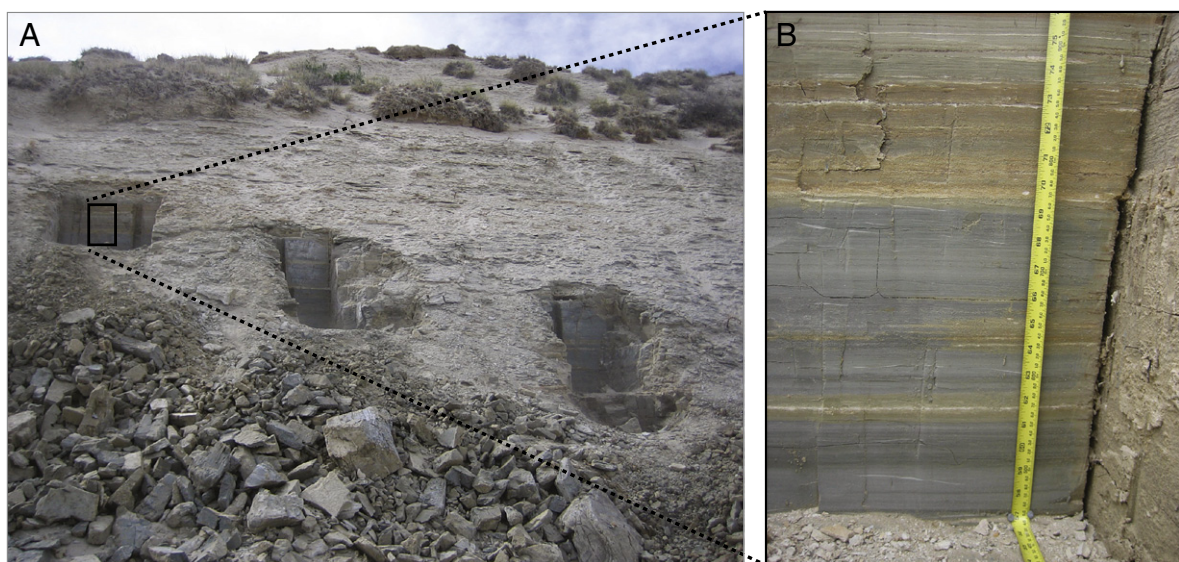


Figure 3. A) Three vertically overlapping trenches were dug in the wall of the Laguna del Perro deflation basin to access LGM sediments; total LGM section thickness at this location is ~1.55 m. Black rectangle shows the location of photo in part b of the figure. B) Photograph of the back wall of the upper trench prior to sampling. Bright white and tan colored layers contain abundant gypsum and are well laminated. Bluish-gray sediments are dominantly carbonate and are frequently mottled, showing evidence of bioturbation. Tape measure shows that transitions between gypsum rich and gypsum poor sediments occur over 1–2 cm, which corresponds to ~35 to 70 yr according to radiocarbon age control.

hexametaphosphate and subjected to 5 s of ultrasonic treatment to remove marl filling the valves. The samples were thoroughly rinsed with deionized water, dried, and picked again using the vacuum extraction line. With the exception of one sample (discussed below), this process yielded samples that were approximately 95% ostracodes or ostracode valve fragments, which were sent to the Center for Accelerator Mass Spectrometry at Lawrence Livermore National Laboratory for dating. Two sieve size fractions, 125 μm and 250 μm , were dated. Additional chronologic control comes from ostracode radiocarbon dates acquired at the top and bottom of the sequence (the *Pisidium* layer and D/E zone transition mentioned earlier) in an adjacent playa (E-19, Fig. 1A) and reported in Allen and Anderson (2000).

Radiocarbon ages were converted to calendar ages using Richard Fairbanks' website at Columbia University (<http://radiocarbon.ldeo.columbia.edu/research/radcarcal.htm>, Fairbanks et al., 2005). Calendar ages were plotted against sample elevation and the resulting best-fit line used to compute an age for each 1-cm sample. Time series of various mineralogical components were analyzed in REDFIT (Schulz and Mudelsee, 2002) in order to identify regular oscillations. REDFIT uses the Lomb–Scargle Fourier transform, which allows for the analysis of irregularly spaced data and is therefore well suited to paleoclimatic data in which changes in sedimentation rate and in ^{14}C production lead to non-uniform time intervals. In my use of REDFIT, I employed a variety of spectral windows (rectangular, Welch, Hanning, triangular, and Blackman–Harris), overlapping segments, and oversampling factors to analyze the data. The average sampling interval of ~ 35 yr gives a Nyquist frequency of $\sim 0.014/\text{yr}$, and plots of the power spectrum and associated statistical confidence lines were therefore truncated at this value.

Results

X-ray diffraction analyses of the LGM sediments reveal that they are composed primarily of calcite, quartz, gypsum/anhydrite, and clays (illite, montmorillonite, and kaolinite), with minor amounts (generally $<5\%$ each) of feldspars (orthoclase, albite, and anorthite) and epsomite, a hydrous magnesium sulfate mineral commonly found in association with gypsum. Based on previous work, I interpret the quartz, clays, and feldspars to be detrital inputs washed into Lake Estancia from the surrounding drainage basin and the gypsum/anhydrite and epsomite to result from the precipitation of evaporite crusts in saline mudflats surrounding the contracted lake during lowstands (Allen and Anderson, 2000; Warren, 2006, p. 178). Microscopic examination shows that calcite exists both in the form of the ostracode valves and as marl filling and surrounding those valves. There is no evidence of detrital limestone.

Two end-member X-ray diffraction patterns exist, one with high gypsum (Fig. 4A) or anhydrite peaks and the other without (Fig. 4B). Rietveld analyses of the binary mixtures of mineral standards yielded weight percentages within 5% of the true values (Table 1), giving confidence that the Rietveld method can be used to track changes in mineral abundance that reflect lake level oscillations. Given the similarity in behavior of the standards containing anhydrite to those containing gypsum, I consider anhydrite to faithfully reflect the gypsum abundance prior to sample heating. While I am aware that this may introduce error in the results since gypsum and anhydrite have somewhat different densities, the results in Table 1, with Rietveld-determined abundances within 5% of actual values, indicate that such an error is small and unlikely to interfere with interpretations of mineralogical trends.

Table 2 gives the radiocarbon ages acquired throughout the LGM sequence. Previously reported dates on modern brine shrimp eggs collected from two different deflation basins yielded modern and 130 ± 65 ^{14}C yr BP dates, suggesting a minimal reservoir effect for groundwater debouching into the lake (Menking and Anderson, 2003). In addition, the very shallow depth of the LGM lake in relation to its surface area, combined with very strong winds in the basin, argues

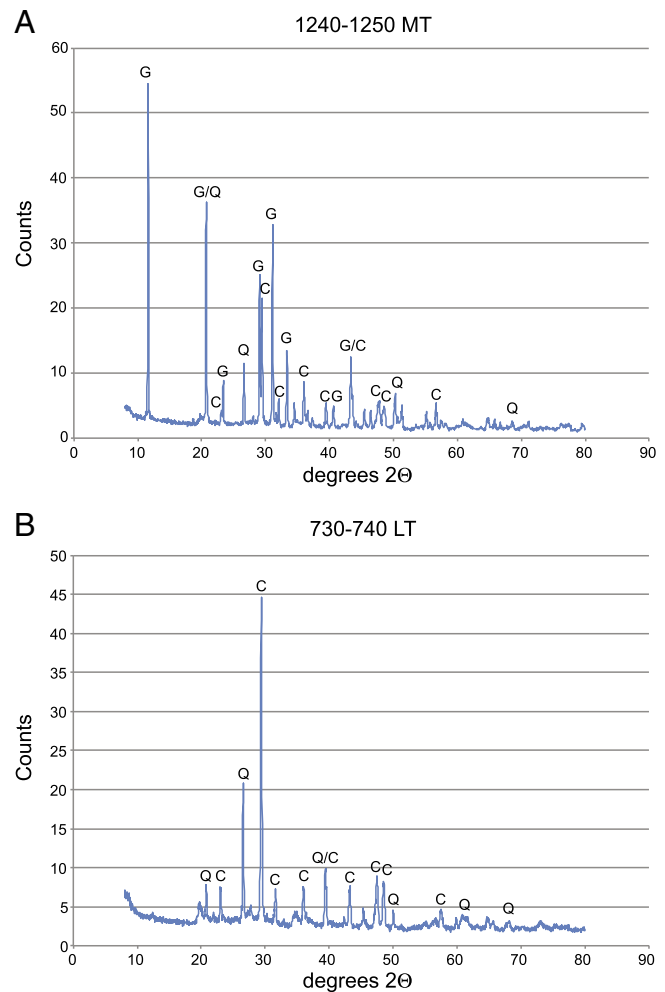


Figure 4. Typical X-ray diffraction patterns of samples containing A) abundant gypsum, and B) very little gypsum. Graph titles are sample names. MT refers to middle trench, whereas LT refers to lower trench. Numbers in sample names refer to the elevation, in mm, above the base of the LGM section. Labeled peaks are associated with gypsum (G), calcite (C), and quartz (Q).

for wind-driven mixing and equilibrium with atmospheric CO_2 during that time. As such, little reservoir effect is expected, and no corrections have been employed in reporting the present dates.

The 250 and 125 μm sieve fractions from each sample (64, 101, and 120 cm above the base of the sequence) newly dated for this study yielded different results, with the 125- μm fraction older than the 250- μm fraction in each case (Table 2). The 125- μm fraction of the 120 cm sample yielded a date that was out of stratigraphic order, and

Table 1

Standard mineral mixtures used to assess accuracy of the Rietveld quantitative analysis method.

Mineral	True weight percent	Rietveld determined weight percent
Calcite	50	52.1
Gypsum	50	47.6
Calcite	50	47.9
Quartz	50	52.0
Gypsum	50	53.6
Quartz	50	46.4
Anhydrite	50	45.1
Quartz	50	54.8

Table 2
Radiocarbon ages for LGM sediments.

^{14}C age (^{14}C yr BP)	Calibrated age (cal yr BP)	Lab number	Material	Locality (playa, elevation)	Source
20,080 ± 100	23,987 ± 130	CAMS-16602	Ostracodes	E-19, base of LGM section	Allen and Anderson, (2000)
17,160 ± 70	20,336 ± 81	CAMS-167282	Ostracodes, 250 μm sieve fraction	Laguna del Perro, 64 cm above base	This paper
18,140 ± 80	21,577 ± 157	CAMS-167283	Ostracodes, 125 μm sieve fraction	Laguna del Perro, 64 cm above base	This paper
16,520 ± 70	19,633 ± 94	CAMS-167284	Ostracodes, 250 μm sieve fraction	Laguna del Perro, 101 cm above base	This paper
17,665 ± 50	20,903 ± 105	CAMS-167340	Ostracodes, 125 μm sieve fraction	Laguna del Perro, 101 cm above base	This paper
16,100 ± 70	19,230 ± 103	CAMS-167285	Ostracodes, 250 μm sieve fraction	Laguna del Perro, 120 cm above base	This paper
20,290 ± 140 ^a	24,197 ± 152	CAMS-167341	Ostracodes, 125 μm sieve fraction	Laguna del Perro, 120 cm above base	This paper
15,130 ± 80	18,343 ± 163	CAMS-4099	Ostracodes	E-19, top of LGM section	Allen and Anderson, (2000)

^a Rejected date.

microscopic inspection of this sample showed it to be full of oogonia of Chara that could not be separated from the ostracode valves. I therefore rejected this date prior to constructing two alternative age models (Fig. 5). In the first (referred to here as the linear age model), I rejected both dates from the 120 cm stratigraphic level and fit a straight line to the remaining six dates. This decision appears justified based on the fact that all of the dates are in stratigraphic order and that the best-fit age model line (calendar age in years = $-35.184 * \text{elevation above the base of the section in cm} + 23,629$) lies between the 125 and 250 μm sieve fraction dates for both newly dated samples (64 and 101 cm stratigraphic levels) when they are plotted in conjunction with the previously reported dates from Allen and Anderson (2000).

In the second age model (referred to here as the polynomial age model), I rejected all of the 125-μm sieve fraction dates and employed a second order polynomial fit to the remaining dates. This decision is justified based on the fact that the 250-μm sieve fraction contained primarily whole ostracode valves, in keeping with the material dated by Allen and Anderson (2000), whereas the 125-μm sieve fraction contained valve fragments that may represent some older, reworked materials.

Figure 6 shows the percentage abundances of detrital minerals, calcite, and evaporites as a function of time using the linear age model.

Detrital inputs vary between ~25 and 70% of the total sediment mass and are most abundant at the beginning of the section, a time of marked lake expansion previously identified by Allen and Anderson (2000) from ostracode assemblages and other evidence. Calcite abundance ranges from ~15 to 50%, and evaporites vary between ~3 and 55% throughout the sequence. Both calcite and detrital inputs to the lake are low at times when evaporite contributions are high, but these same components are inversely abundant when evaporite concentrations are low. Several prominent low intervals in evaporite abundance from ~23,600–23,400, ~21,500–21,300, ~20,300–19,800, ~19,500–18,900, and ~18,500–18,300 yr BP appear to correlate with previously reported highstands of Lake Estancia (Fig. 6; Allen and Anderson, 2000).

Visual inspection of all three mineralogic components shows that they demonstrate large (10–50% changes in concentration) centennial and millennial scale oscillations in abundance. Figures 7 and 8 show the results of spectral analyses performed on the different series to determine the periods of these oscillations. Several spectral peaks meet or exceed the 90% confidence interval, with some variability in peak significance depending on the age model and choice of analysis parameters used (e.g. spectral window shape, number of overlapping segments, oversampling factor). For the linear age model (Fig. 7), the

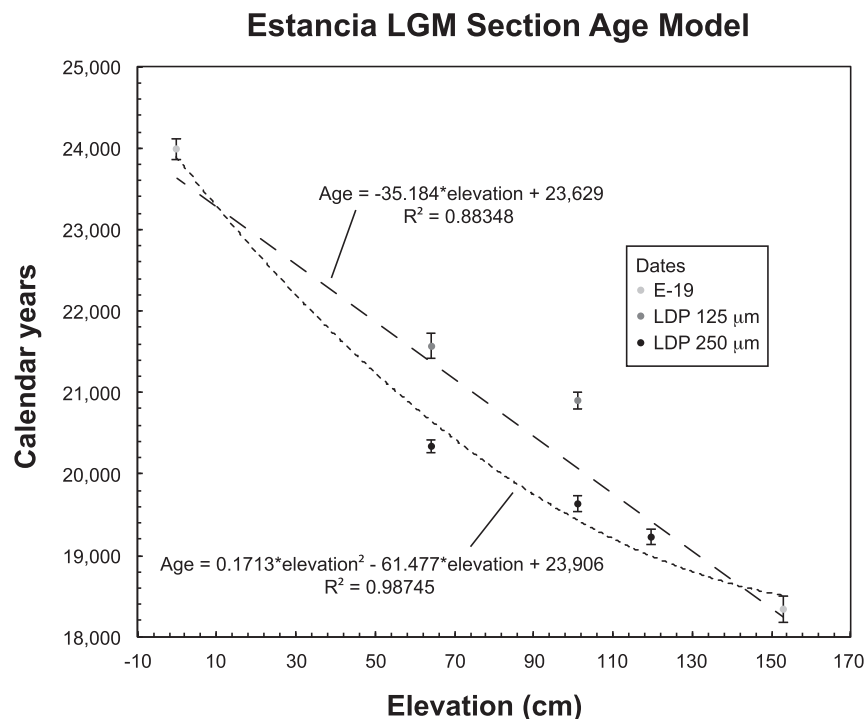


Figure 5. Age models for the Estancia LGM sequence. The linear model (long dash) includes both the 125 and 250 μm dates for the samples at 64 and 101 cm above the base of the section as well as the Allen and Anderson (2000) dates at the boundaries of the section. The polynomial model (short dash) uses all three 250 μm dates newly acquired for this paper along with those of Allen and Anderson (2000).

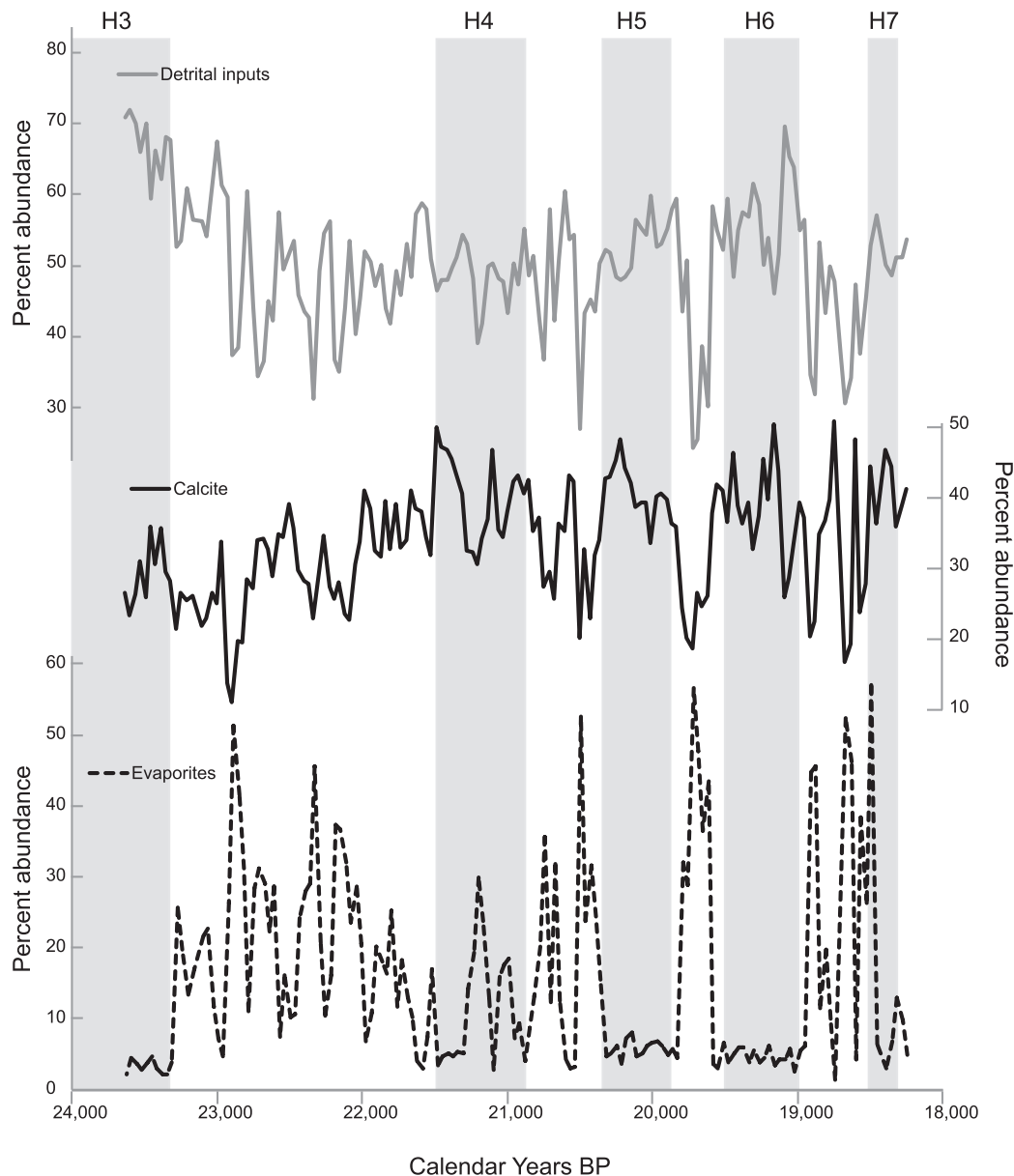


Figure 6. Percentages of detrital mineral inputs from the Estancia Basin, calcite precipitated both inorganically and biogenically within Lake Estancia, and evaporite minerals blown into the lake from surrounding mudflats as a function of time (linear age model). Detrital inputs consist of the sum of quartz, clays, and feldspars. Evaporites consist of the sum of gypsum, anhydrite, and epsomite. Gray bars behind the percentage abundance graphs show the timing of lake highstands labeled H3 through H7 by Allen and Anderson (2000). H3 and H5–H7 correspond to radiocarbon-dated (ostracodes) highstand shoreline deposits and correlate to periods of low evaporite abundance in the present record. The existence of H4 was inferred from basin-center stratigraphic evidence; highstand shoreline deposits of this age have not been identified, and only part of the present record shows low evaporite concentrations during this period.

evaporite series shows prominent peaks at ~900, ~375, ~265, 88, and 80 yr, some of which also appear in the calcite series. In the detrital series, the most significant spectral peaks are associated with periods of ~255 and 88 yr, with less significant peaks at 96 and 81 yr depending on the choice of window shape and size employed in the analysis. An ~200 to 250-yr spacing in detrital quartz peaks during the LGM was previously identified by Allen and Anderson (1993) and attributed to abrupt increases in winter moisture that led to lake freshening events with attendant changes in ostracode species distributions.

The spectral analysis using the polynomial age model (Fig. 8) shows prominent peaks in all three mineralogical components at ~270 yr, with less significant peaks in the range of 97–77 yr. All three series show peaks at around 200 yr, but only in the evaporites and one of the detrital analyses do these peaks rise above the 80% confidence interval, making the existence of this period suspect. All three series show strong

(90% + confidence interval) spectral peaks in the 500–600-yr range, but the periods associated with these peaks show fairly broad scatter between different analysis parameters and different mineralogical components.

Discussion

Several of the spectral peaks identified by REDFIT are consistent with or quite similar to ones associated with known solar forcing. Regardless of spectral window parameters used, the evaporite and detrital series fit with the linear age model each show a highly significant peak (>95% confidence interval) at a frequency of 0.0114/yr, corresponding to a period of 88 yr (Fig. 7). Peaks of similar period but of lower significance are seen in the polynomial age model results. The 88-yr period is consistent with the Gleissberg cycle, a modulation of the amplitude of the 11-

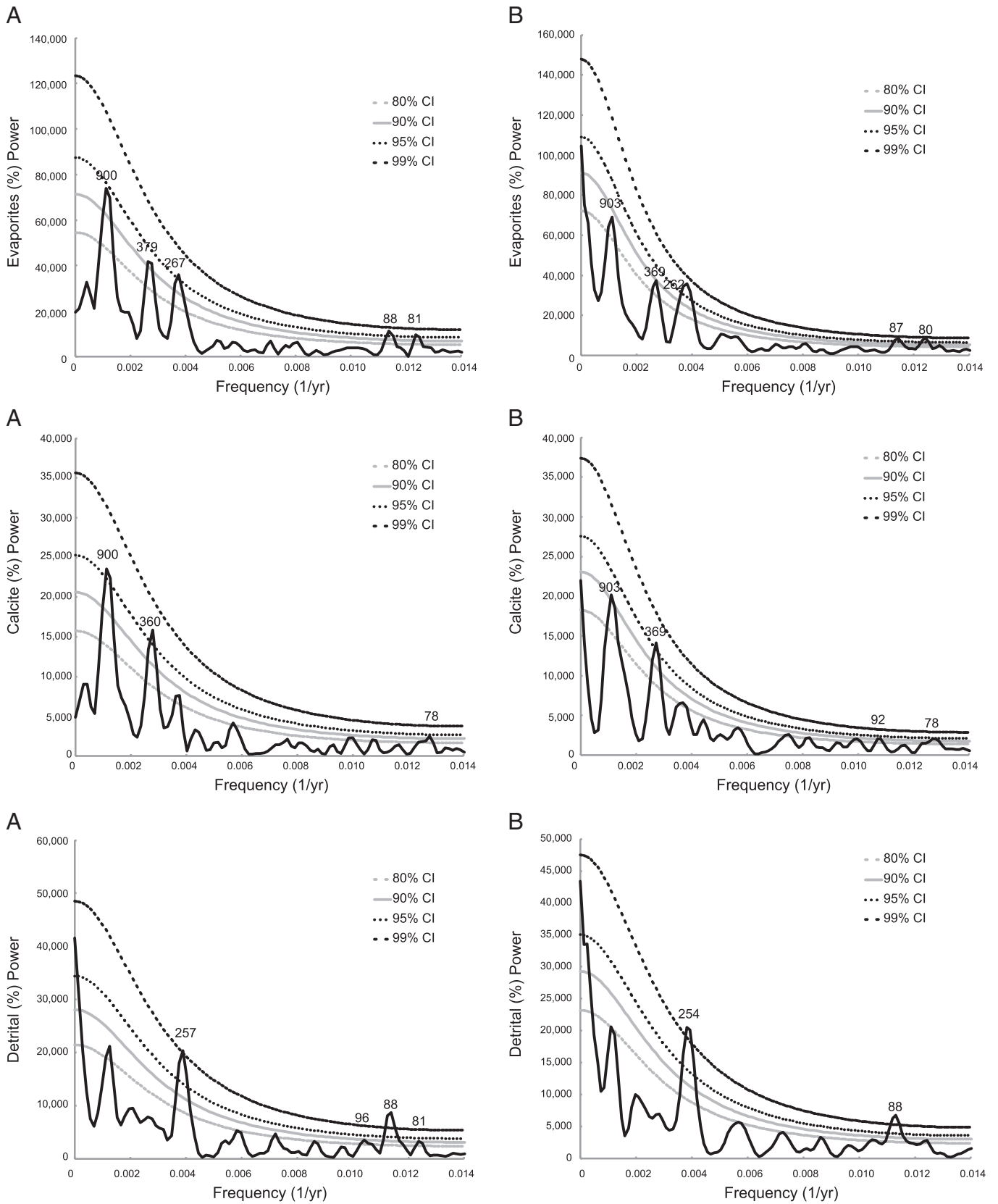


Figure 7. Power spectra of evaporite (top), calcite (middle), and detrital (bottom) abundances (solid black lines) as computed by REDFIT (Schulz and Mudelsee, 2002) and using the linear age model. Confidence intervals (CI) shown by different dashed, dotted, and solid gray and black lines. Peaks labeled according to the period of oscillation they represent, in years. A) Two 50% overlapping triangular windows used with an oversampling factor of 2. B) Three 50% overlapping Welch windows used with an oversampling factor of 3.

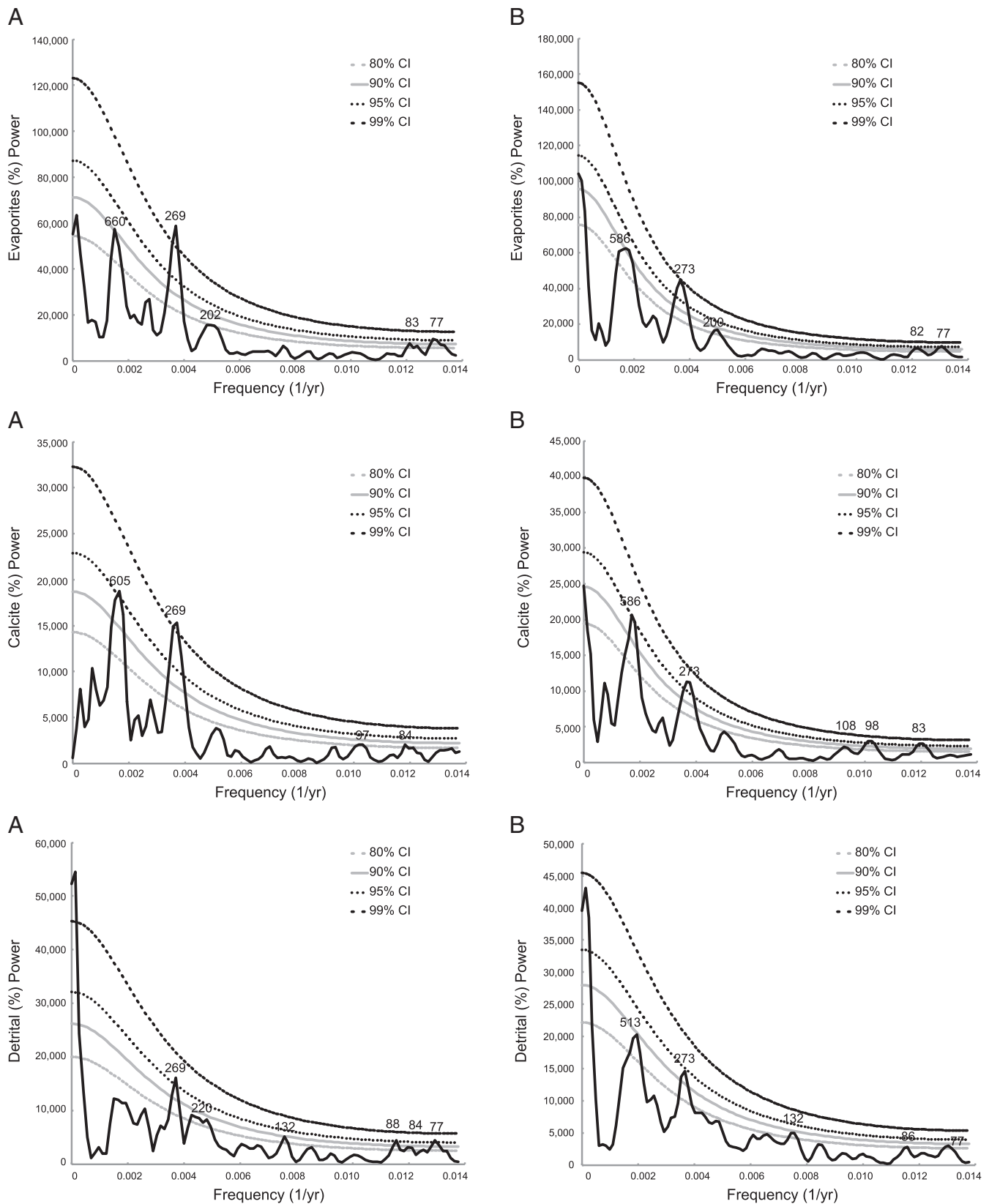


Figure 8. Power spectra of evaporite (top), calcite (middle), and detrital (bottom) abundances (solid black lines) as computed by REDFIT (Schulz and Mudelsee, 2002) and using the polynomial age model. See caption for Fig. 7 for further explanation.

yr Schwabe sunspot cycle that shows up repeatedly in the radiocarbon record from Holocene tree-ring series (Peristykh and Damon, 2003; Braun and Kurths, 2010) in addition to the direct observation of

sunspots since AD 1700 and in the frequency of solar aurorae since the 4th century AD. Strong spectral peaks at 900 yr, 365–375 yr and 255–273 yr (Figs. 7, 8) are similar to periods of 940 yr, 360 yr,

352–357 yr and 286–300 yr in the $\Delta^{14}\text{C}$ record reported by Stuiver and Braziunas (1989), Damon and Jirikowic (1992), Damon and Peristykh (2000), Vasiliev and Dergachev (2002) and Clemens (2005) that have been attributed to harmonics of a ~2100–2400-yr Hallstattzeit period in solar forcing (Damon and Jirikowic, 1992; Soon et al., 2014).

Both Stuiver and Braziunas (1993) and Clemens (2005) reported ~500–525 yr cycles in the early Holocene portion of the long-term $\Delta^{14}\text{C}$ record, which the latter attributed to variations in North Atlantic Deep Water formation brought about by changing glacial meltwater fluxes that would in turn have changed rates of upwelling and ventilation of ^{14}C depleted deep water to the atmosphere. These periods are similar to the 513–586-yr period seen in the Estancia sediments when the polynomial age model is used (Fig. 8), though, as noted, their connection to solar activity is unclear. I have found no evidence in the Estancia LGM sediments for 703–717-yr cycles identified in the long-term $\Delta^{14}\text{C}$ record (Clemens, 2005), and only a very weak ($\leq 80\%$ confidence interval, Fig. 8) suggestion in the polynomial age model results of the ~210-yr Suess/DeVries solar cycle common in the long-term $\Delta^{14}\text{C}$ record and cosmogenic radionuclide records from ice cores (Steinhilber et al., 2012).

A number of studies of late Pleistocene and Holocene climates in New Mexico and Colorado may help to explain the decadal to millennial variability exhibited in the Estancia LGM record of mineralogical fluctuations. Asmerom et al. (2010) found evidence for Dansgaard–Oeschger and Heinrich events in oxygen isotopic values in a speleothem from Ft. Stanton Cave in the Guadalupe Mountains of southeastern New Mexico, which lies in the same general latitude belt as the Estancia Basin. Correlations to the GRIP ice core over the interval ~10 to 60 ka revealed that climatic warmings in Greenland were associated with a shift to drier climate in New Mexico, whereas colder conditions in Greenland led to wetter conditions. Further comparison of the Ft. Stanton record to isotopic variations measured in a speleothem from Hulu Cave, China, showed that the two series were anti-phased, with wetter conditions at Ft. Stanton corresponding to drier conditions at Hulu Cave. Asmerom et al. (2010) suggested that latitudinal shifts in the position of the polar jet stream and intertropical convergence zone (ITCZ) could explain the opposite behavior of the two records and would change the relative importance of winter Pacific cyclones versus summer monsoonal precipitation at Ft. Stanton. Inasmuch as the Hulu Cave $\delta^{18}\text{O}$ series is thought to be a record of the strength of the East Asian monsoon (Wang et al., 2001), a weaker monsoon in China appears to be correlated with higher winter precipitation rates in central New Mexico, a potential mechanism by which solar variability might be translated into precipitation changes in the American Southwest.

Additional records from the region implicate solar activity as a source of climatic variability. For example, Jiménez-Moreno et al. (2008) found evidence for centennial- and millennial-scale cycles in late Pleistocene and Holocene sediments from alpine Stewart Bog in the Sangre de Cristo Mountains of northern New Mexico (Fig. 1). Spectral and cross-spectral analyses of the percentage of arboreal pollen, the ratio of *Picea* to *Artemisia* pollen, and magnetic susceptibility revealed cycles ~200 yr in length that they attributed to temperature-induced variations in the position of the tree line and tentatively correlated to the Suess/DeVries solar cycle. Additional periods of ~300, 531, 793, and 1592 yr appear similar to cycles previously identified as having a solar origin by Damon and Sonnett (1991) and recognized variously in sediments from the North Atlantic (Bond et al., 2001 ascribed a 1500-yr cycle in ice rafted debris to variations in solar irradiance) and Gulf of Mexico (Poore et al., 2003 attributed 550, 300, 250, 230, 212, and 170-yr cycles in abundance of *Globigerinoides sacculifer* to solar activity). High-resolution pollen, charcoal, organic carbon, and carbon isotopic analyses of sediments from a lake in northern Colorado yielded similar results (Jiménez-Moreno et al., 2011).

Farther south in New Mexico, Asmerom et al. (2007) measured $\delta^{18}\text{O}$ values on a Holocene speleothem from Pink Panther Cave in the Guadalupe Mountains and found decadal-, centennial-, and millennial-scale

variations that they attributed to changes in overall annual moisture balance and that have spectral peaks consistent with previously recognized periods in the $\Delta^{14}\text{C}$ record (Stuiver and Braziunas, 1993). More negative $\delta^{18}\text{O}$ values were ascribed to either a greater amount of winter precipitation from Pacific frontal storms, greater summer precipitation from the North American Monsoon (with the amount effect called on to reduce $\delta^{18}\text{O}$ value), or both, and more positive $\delta^{18}\text{O}$ values to a reduction in precipitation from these sources. In addition, the $\delta^{18}\text{O}$ record from the Pink Panther Cave appears to be anti-correlated to $\Delta^{14}\text{C}$, meaning that intervals of lower solar activity corresponded to wetter climates while higher solar activity was associated with drying.

The appearance of several cycles in mineral abundance in the Estancia LGM sediments suggests a mechanism whereby Lake Estancia experienced repeated abrupt oscillations in volume during the LGM. If variations in solar irradiance gave rise to variations in the strength of the East Asian monsoon with associated teleconnections to precipitation rates in New Mexico (Asmerom et al., 2010, mechanism), the Estancia Basin would have experienced pulsating changes in winter rainfall and snowmelt over time. Inasmuch as isotopic evidence (Menking and Anderson, 2003) demonstrates that stream flow and groundwater recharge in the basin are dominated by winter precipitation, these pulses would have manifested themselves in changing lake levels. The time series of detrital mineral influxes to the lake (Fig. 6) is the most sensitive recorder of these pulses and shows cycles of ~260 and 88 yr. An ~900-yr cycle appears responsible for the previously identified (Allen and Anderson, 2000) millennial-scale oscillations shown in Figures 1C and 6, and constructive interference with shorter ~365, ~260, and 88-yr cycles may explain the rapidity with which the lake expanded and contracted between its highstand and lowstand levels. The Gleissberg-scale and 260-yr oscillations in particular are of an appropriate period to quickly boost rain- and snow-fall rates, allowing the lake to expand, while then reversing direction and preventing basin overflow as other longer cycles reached their peak values. Such a mechanism may also provide an alternative or additional explanation for the repeated stabilization of the lake at a common highstand elevation.

Conclusions

This study sought a mechanism to explain very rapid (decades) and large changes in the lake level in the Estancia Basin during Last Glacial Maximum time. Spectral analysis of mineralogical time series that serve as proxies for stream flow and overall hydrologic balance yield periods consistent with solar forcing at decadal, centennial, and millennial timescales. While baseline climatic conditions in central New Mexico are obviously quite different today, identification of cycles consistent with solar forcing is important to our understanding of anthropogenic climate change in the region. Given that these cycles are external to the Earth's climate system, we might anticipate that they continue to influence hydrological processes and may combine with changes in rainfall and runoff rates associated with global warming to affect hydrological balance in the future. That two of the observed cycles operate near centennial time-scales may also confound our abilities to tease apart natural and anthropogenic contributions to ongoing climatic change.

Acknowledgments

I would like to thank Roger Anderson, Joshua Faulconer, Wesley Labor, and Cara Hunt for their assistance with sample collection. Aaron Jones and students from the spring 2012 Vassar College Paleoclimatology course (Danielle Bonneau, David de la Torre, Alison Denn, Patrick Donohue, Laura Gruenberg, Ian Heller, Gary Linkevich, Alison Mooradian, Andrew Rock, Michael Sandstrom, Jeremy Snailer, Sophia Wassermann, and Joseph Wheeler) performed additional sample processing. I also thank Jeff Walker for his assistance with the X-ray diffractometer, Alan Coelho, John Evans, and Nathan Henderson for

their help with Rietveld refinement, and Manfred Mudelsee and Michael Schulz for suggestions on how to best use REDFIT. Tom Guilderson at the LLNL-CAMS performed the radiocarbon dating. Funding for this project came from the National Science Foundation's Major Research Instrumentation program, award #1229257, and the Priscilla Bullitt Collins Environmental Science Faculty Research Fund at Vassar College. Finally, I would like to thank Gonzalo Jiménez-Moreno and an anonymous reviewer for helpful reviews that improved the manuscript.

References

- Allen, B.D., Anderson, R.Y., 1993. Evidence from Western North America for rapid shifts in climate during the Last Glacial Maximum. *Science* 260, 1920–1923.
- Allen, B.D., Anderson, R.Y., 2000. A continuous, high-resolution record of late Pleistocene climate variability from the Estancia Basin, New Mexico. *Geological Society of America Bulletin* 112, 1444–1458.
- Anderson, R.Y., Allen, B.D., Menking, K.M., 2002. Geomorphic expression of abrupt climate change in southwestern North America at the glacial termination. *Quaternary Research* 57, 371–381.
- Asmerom, Y., Polyak, V., Burns, S., Rasmussen, J., 2007. Solar forcing of Holocene climate: new insights from a speleothem record, southwestern United States. *Geology* 35, 1–4.
- Asmerom, Y., Polyak, V., Burns, S.J., 2010. Variable winter moisture in the southwestern United States linked to rapid glacial climate shifts. *Nature Geoscience* 3, 114–117.
- Ault, T.R., Cole, J.E., Overpeck, J.T., Pederson, G.T., Meko, D.M., 2014. Assessing the risk of persistent drought using climate model simulations and paleoclimate data. *Journal of Climate* 27, 7529–7549.
- Bachhuber, 1971. Paleolimnology of Lake Estancia and the Quaternary History of the Estancia Valley. (Ph.D. dissertation), University of New Mexico, central New Mexico (238 pp.).
- Benson, L.V., Currey, D.R., Dorn, R.I., Lajoie, K.R., Oviatt, C.G., Robinson, S.W., Smith, G.J., Stine, S., 1990. Chronology of expansion and contraction of four Great Basin lake systems during the past 35,000 years. *Palaeogeography, Palaeoclimatology, Palaeoecology* 78, 241–286.
- Bish, D.L., Howard, S.A., 1988. Quantitative phase analysis using the Rietveld method. *Journal of Applied Crystallography* 21, 86–91.
- Bish, D.L., Post, J.E., 1993. Quantitative mineralogical analysis using the Rietveld full-pattern fitting method. *American Mineralogist* 78, 932–940.
- Bond, G., Kromer, B., Beer, J., Muscheler, R., Evans, M.N., Showers, W., Hoffmann, S., Lott-Bond, R., Hajdas, I., Bonani, G., 2001. Persistent solar influence on North Atlantic climate during the holocene. *Science* 294, 2130–2136.
- Braun, H., Kurths, J., 2010. Were Dansgaard–Oeschger events forced by the sun? *The European Physical Journal Special Topics* 191, 117–129.
- Clemens, S.C., 2005. Millennial-band climate spectrum resolved and linked to centennial-scale solar cycles. *Quaternary Science Reviews* 24, 521–531.
- Damon, P.E., Jirlikowic, J.L., 1992. The sun as a low-frequency harmonic oscillator. *Radiocarbon* 34, 199–205.
- Damon, P.E., Peristykh, A.N., 2000. Radiocarbon calibration and application to geophysics, solar physics, and astrophysics. *Radiocarbon* 42, 137–150.
- Damon, P.E., Sonnett, C.P., 1991. Solar and terrestrial components of the atmospheric ^{14}C variation spectrum. In: Sonnett, C.P., Giampapa, M.S., Matthews, M.S. (Eds.), *The Sun in Time*. University of Arizona Press, Tucson, pp. 360–388.
- Downs, R.T., Hall-Wallace, M., 2003. The American mineralogist crystal structure database. *American Mineralogist* 88, 247–250.
- Fairbanks, R.G., Mortlock, R.A., Chiu, T.-C., Cao, L., Kaplan, A., Guilderson, T.P., Fairbanks, T.W., Bloom, A.L., Grootes, P.M., Nadeau, M.-J., 2005. Radiocarbon calibration curve spanning 0 to 50,000 years BP based on paired $^{230}\text{Th}/^{234}\text{U}/^{238}\text{U}$ and ^{14}C dates on pristine corals. *Quaternary Science Reviews* 24, 1781–1796.
- Jiménez-Moreno, G., Fawcett, P.J., Anderson, R.S., 2008. Millennial- and centennial-scale vegetation and climate changes during the late Pleistocene and Holocene from northern New Mexico (USA). *Quaternary Science Reviews* 27, 1442–1452.
- Jiménez-Moreno, G., Anderson, R.S., Atudorei, V., Toney, J.L., 2011. A high-resolution record of climate, vegetation, and fire in the mixed conifer forest of northern Colorado, USA. *GSA Bulletin* 123, 240–254.
- Kutzbach, J.E., Wright, H.E., 1985. Simulation of the climate of 18,000 years BP: results for the North American/North Atlantic/European sector and comparison with the geological record of North America. *Quaternary Science Reviews* 4, 147–187.
- Leopold, L.B., 1951. Pleistocene climate in New Mexico. *American Journal of Science* 249, 152–168.
- Menking, K.M., Anderson, R.Y., 2003. Contributions of La Niña and El Niño to middle Holocene drought and late Holocene moisture in the American Southwest. *Geology* 31, 937–940.
- Menking, K.M., Anderson, R.Y., Shafike, N.G., Syed, K.H., Allen, B.D., 2004. Wetter or colder during the Last Glacial Maximum? Revisiting the pluvial lake question in southwestern North America. *Quaternary Research* 62, 280–288.
- Peristykh, A.N., Damon, P.E., 2003. Persistence of the Gleissberg 88-year Solar Cycle Over the Last ~12,000 Years: Evidence From Cosmogenic Isotopes. *Journal of Geophysical Research-Space Physics* 108. <http://dx.doi.org/10.1029/2002JA009390>.
- Phillips, F.M., Campbell, A.R., Kruger, C., Johnson, P., Roberts, R., Keyes, E., 1992. A reconstruction of the response of the water balance in western United States lake basins to climatic change. New Mexico Water Resources Research Institute report 269.
- Poore, R.Z., Dowsett, H.J., Verardo, S., 2003. Millennial- to century-scale variability in Gulf of Mexico Holocene climate records. *Paleoceanography* 18. <http://dx.doi.org/10.1029/2002PA000868>.
- Schulz, M., Mudelsee, M., 2002. REDFIT: estimating red-noise spectra directly from unevenly spaced paleoclimatic time series. *Computers and Geosciences* 28, 421–426.
- Soon, W., Velasco Herrera, V.M., Selvarag, K., Traversi, R., Usoskin, I., Chen, C.-T.A., Lou, J.-Y., Kao, S.-J., Carter, R.B., Pipin, V., Severi, M., Becagli, S., 2014. A review of Holocene solar-linked climatic variation on centennial to millennial timescales: physical processes, interpretive frameworks and a new multiple cross-wavelet transform algorithm. *Earth-Science Reviews* 134, 1–15.
- Steinhilber, F., Abreu, J.A., Beer, J., Brunner, I., Christl, M., Fischer, H., Heikkilä, U., Kubik, P.W., Mann, M., McCracken, K.G., Miller, H., Miyahara, H., Oerter, H., Wilhelms, F., 2012. 9400 years of cosmic radiation and solar activity from ice cores and tree rings. *Proceedings of the National Academy of Sciences* 109, 5967–5971.
- Stuiver, M., Braziunas, T.F., 1989. Atmospheric ^{14}C and century-scale solar oscillations. *Nature* 338, 405–408.
- Stuiver, M., Braziunas, T.F., 1993. Sun, ocean, climate and atmospheric $^{14}\text{CO}_2$: an evaluation of causal and spectral relationships. *The Holocene* 3, 289–305.
- Vasiliev, S.S., Dergachev, V.A., 2002. The ~2400-year cycle in atmospheric radiocarbon concentration: bispectrum of ^{14}C data over the last 8000 years. *Annales Geophysicae* 20, 115–120.
- Wang, Y.J., Cheng, H., Edwards, R.L., An, Z.S., Wu, J.Y., Shen, C.-C., Dorale, J.A., 2001. A high-resolution absolute-dated late Pleistocene monsoon record from Hulu Cave, China. *Science* 294, 2345–2348.
- Warren, J.K., 2006. *Evaporites: Sediments, Resources and Hydrocarbons*. Springer-Verlag, Berlin.
- Wilkins, D.E., Currey, D.R., 1997. Timing and extent of late Quaternary paleolakes in the Trans-Pecos closed basin, west Texas and south-central New Mexico. *Quaternary Research* 47, 306–315.
- Young, R.A., 1993. Introduction to the Rietveld method. In: Young, R.A. (Ed.), *The Rietveld Method*. Oxford University Press.
- Zhang, W., Wu, J., Wang, Y., Wang, Y., Cheng, H., Kong, X., Duan, F., 2014. A detailed East Asian monsoon history surrounding the 'Mystery Interval' derived from three Chinese speleothem records. *Quaternary Research* 82, 154–163.